Analyzing Di-Electric Properties of $ZnTio_3$ Nano Particles

Srinivasa S.[1], Dr. Vipin Kumar[2]

[1]Research Scholar, OPJS University, Churu, Rajasthan
[2]Professor, OPJS University, Churu, Rajasthan

Abstract

$ZnTiO_3$ nano powders were obtained by sol-gel method. The nano powders were characterised by means of TGA/DTA analysis, X-ray diffraction, TMA analysis and SEM characterization. The results show that the crystalline structure of the sol-gel powders was obtained at 600 °C, with crystallite sizes of 10 nm. SEM shows that most of the prepared $ZnTiO_3$ nano powders are agglomerated. Since agglomeration plays an important role in the sintering of the $ZnTiO_3$ ceramics, different deagglomeration techniques (ultrasonication, pulverization and attrition milling) were investigated. Dense $ZnTiO_3$ structure was obtained from the attrition milled powder at 1050 °C and its dielectric characteristics were also investigated (εr =25, tε= -26 ppm/°C and tgδ < 10-3 at 1 MHz). The low sintering temperature and the good dielectric properties show promise for the manufacture of multilayered capacitors with internal copper electrodes.

Keywords: *Bacatio, Dielectric Properties, Structure, Permittivity, Dielectric Tunability.*

1. INTRODUCTION

Electromagnetic and microwave radiation pollutions are becoming a major issue as the use of contemporary communication technology and electronic gadgets continues to grow. Because of this, more and more research is being done on producing antiradiation and microwave absorbing materials. Magnetic losses at gigahertz frequencies make magnetoplumbite hexaferrites ideal for electromagnetic interference suppression and radar absorbent materials. There are six distinct sorts of hexagonal structures, namely M, W, X, Y, Z, and U, for the hexagonal structure. S ($2MFe_2O_4$), R ($Sr/Sr\ Fe_6O_{11}$) and/or T ($(Ba/Sr)_2\ Fe_8O_{14}$) blocks in the complex hexaferrites are all structurally distinct, but the Gibbs free energy of their synthesis and the thermodynamic conditions for their creation are all the same. It is possible that the reaction mixtures for which the stoichiometry of a certain Hexaferrite is used may result in the creation of another Hexaferrite with a slightly different combination of structural blocks. There are many types of hexagonal ferrites that are ideal for microwave absorption, but X-type hexaferrites, which have low coercivity and strong saturation magnetization, are among the most difficult to prepare.

2. LITERATURE REVIEW

Feng Gao et. al, (2021): This paper reviews recent developments and challenges of (Ba, Sr) TiO_3/polymer functional composites. The microstructure of barium-strontium titanate (Ba, Sr) TiO_3(BST)/polymer composites with different polymer matrices and the nature of the interface between the BST and polymer matrix is critical in the final dielectric properties. The effects of concentration, particle size and BST filler shape on the dielectric properties of BST/polymer composites are discussed. A theoretical model for the dielectric constants of ceramic/polymer composites and the fabrication of BST/polymer composites are described briefly. The development of a dielectric tunability for the BST/polymer composites is summarized. A dielectric tunability theoretical model is proposed based on our previous research results and the effects of several factors on the dielectric tunability of the composites are discussed, which contributes to a prediction of the dielectric tunability of the composites and provides important theoretical and research significance for future work.

Jyoti Rani et. al, (2021): Magnetoelectric (ME) heterostructures with strong ME coupling at room temperature are of great importance due to their promising applications in next-generation devices. Here, lead-free [Ba (Zr0.2Ti0.8) O3-0.5(Ba0.7Ca0.3) TiO_3]/$CoFe_2O_4$/ [Ba (Zr0.2Ti0.8) O3-0.5(Ba0.7Ca0.3) TiO3] (abbreviated as (BZT-0.5BCT)/CFO/(BZT-0.5BCT)) trilayer thin film has been deposited on Pt/Ti/SiO_2/Si (100) substrate by pulsed laser deposition technique. Dielectric properties of trilayer thin film show the relaxor behavior and high value of dielectric constant (~2.2 × 103) with low dielectric loss (~0.16) at frequency 100 Hz at room temperature. Typical ferroelectric and magnetic hysteresis loops were found with large electric polarizations (Ps

= 12.14 μC/cm^2, Pr = 6.0 μC/cm^2) and magnetization (Ms = 246 emu/cc and Mr = 66.6 emu/cc), respectively. The change in PE loop on the application of magnetic field represents the strong ME coupling. The high value of ME coefficient (~0.74 V/cm. Oe) was detected at room temperature which indicates its potential application for multifunctional ME devices.

G.M. Rashwan et. al, (2021): (Ba0.95 Ca0.05) TiO3 ceramic was prepared by solid-state reaction method for different calcination temperatures 1100°C, 1150°C, and 1200°C. X-ray Diffraction (XRD) analysis was performed, it shows that the crystallization starts to form at 1200°C. Sintering was carried out at 1400°C for 3 hours. The sample was characterized by transmission electron microscopy (TEM), scan electron microscopy (SEM), and UV-Visible spectrophotometer. Dielectric properties of this sample were measured in the temperature range 25oC - 140oC, which demonstrates that the maximum dielectric constant (Ɛ) =1982. Rietveld refinement analysis for the XRD pattern is performed, which indicated that Ca-ions enter the tetragonal unit cell and replace Ba-ion and maintain the perovskite tetragonal structure.

MD. Parvez Ahmad et. al, (2020): In this paper, Carbon-doped Zinc Oxide (C-ZnO) samples were prepared using the solid-state reaction method. The influence of carbon-doping on the structural and dielectric properties of ZnO samples was studied. The shift in the highest peak position (101) in XRD patterns of carbon-doped samples was observed. The Raman peak at 581cm−1 in undoped ZnO was shifted and broadened in carbon-doped ZnO samples. The ZnO samples doped with carbon show higher values of dielectric constant (~2400 at 1kHz) compared to pure ZnO (~9 at 1kHz) which was due to increase in native point defects in the samples. The ac conductivity (σac) value of the carbon-doped sample was enhanced by 103 times for ((ZnO)0.9C0.1) sample.

Naveen Kumari et. al, (2014): FeCrxFe2−xO4 (x==0.1, 0.2, 0.3, 0.4 and 0.5) nano-particles were synthesized by a chemical co precipitation method and the effect of Cr3+ substitution on structural and dielectric properties of Fe3O4 was studied. Structural studies were carried out using X-ray diffraction (XRD) and transmission electron microscopy (TEM) techniques. XRD pattern confirmed the single spinel ferrite phase formation. Particle size and crystallite size of the synthesized materials lie in the range of 25-50 nm as calculated from electron microscopy images and X-ray diffraction patterns using Scherrer′s formula. Dielectric loss (tanδ), real part of dielectric constant (ε′), imaginary part of dielectric constant (ε″), ac conductivity (σac), real (resistive) part of impedance (Z′) and imaginary part of impedance (Z″) were evaluated as a function of frequency, composition and temperature using an impedance analyzer in the frequency range of (1 kHz-5 MHz) and temperature range of (27-250 °C). AC conductivity (σac) was found to decrease with increase in Cr3+ ion doping and can be explained on the basis of hopping mechanism. The variation of dielectric loss (tanδ), dielectric permittivity (ε′), ac conductivity (σac) with temperature and frequency can be explained on the basis of Maxwell-Wagner type of interfacial polarization and hopping mechanism between ferrous and ferric ions at octahedral site. Variation in Cole-Cole plots with temperature shows decrease in resistivity with increase in temperature. The Nyquist impedance plots of the prepared materials reveals the inherent phenomenon involved in conduction mechanism of Cr3+ substituted Fe3O4 ferrites. Behavior of DC electrical resistivity with increasing temperature indicates that the substituted ferrites have semiconductor like behavior. Activation energy was found to increase with increasing Cr3+ ion content.

3. METHODOLOGY

Sol-gel synthesis (sg-ZT)

The ZnTiO3 gel was synthesised from titanium bu-toxide, Ti(OC4H9)4 (purity of 99.5%). Titanium butoxide was diluted in absolute ethanol (purity of 99.5%) and stirred for 30 minutes. The obtained solution was then added drop wise to the solution containing ethanol, water and a few drops of HNO3 and stirred again for 2 hours in order to prepare a homogeneous solution (solu-tion 1). At the same time solution 2 was prepared by to-tal dissolution of zinc acetate, Zn(OOCCH 3)2 (purity of 99.5%) in ethylene glycol. Finally, solution 2 was added drop wise to solution 1, under stirring, during a period of 1 hour, which led to the formation of a homogeneous gel. The obtained gel was dried at 110 °C for 5 hours, ground in a mortar to produce powder and heat treat-ed in air for 2 hours at various temperatures (600 °C, 700 °C, 800 °C, 900 °C and 1000 °C). The whole pro-cess is schematically presented in Fig. 1.

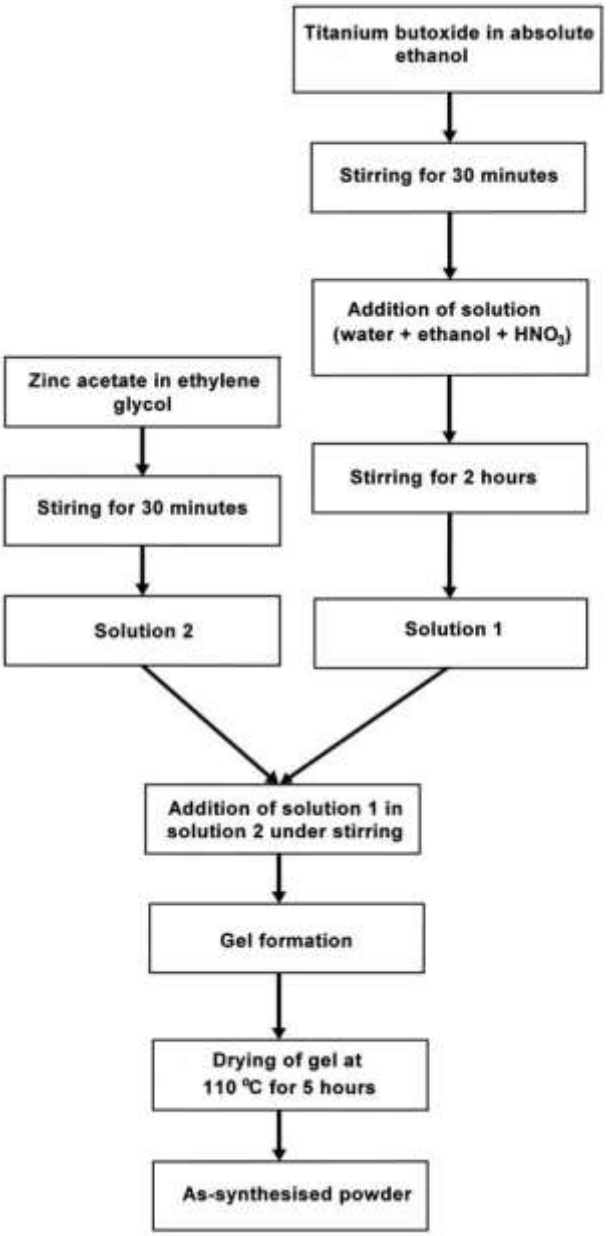

Figure 1. Schematic flow chart of the synthesis of ZnTiO3 powders by sol-gel technique

Solid state synthesis (ss-ZT)

The precursors, ZnO and TiO2 (purity >99%), were appropriately weighted according to the Zn/Ti = 1 molar ratio. Mixing was performed in an ammonia solution at pH = 11 using zirconia balls in a teflon jar for 3 hours. These conditions were reported to be optimal for obtaining a stable suspension [8,9]. The slurry was subsequently dried and the obtained powder was manual-ly reground and heat treated in air for 2 hours at various temperatures (700 °C, 800 °C, 900 °C and 1000 °C). The powder was finally reground in an ammoniac solution at pH = 11 for 1 hour, as described previously.

Processing of ZnTiO3 ceramics

Pressed pellets (8 or 6 mm in diameter and 2 mm thick) were prepared by uniaxial pressing (at a load of about 21 kN) of the synthesised powders mixed with an organic binder (polyvinyl alcohol at 5 vol.%). The green samples were finally sintered in air in a tubular furnace for two hours at a dwell temperature previously determined by thermo-mechanical analysis and heating and cooling rates of 150 °C/h.

4. ANALYSIS

ZT powder synthesized by sol-gel method

Figure 2 shows TGA/DTA curves of the sol-gel powder and gives the evidence for several phenomena listed below.

- An exothermic peak between 277–358 °C is observed on the DTA curve, accompanied by weight loss of 20 wt.% (TGA curve). This can be attributed to the departure of the organic solvents and the combastion of the organic residues.
- An exothermic peak in the temperature range 320– 380 °C results from the dihydroxylation of Ti-OH into TiO2 [10].
- The weight loss ends around 500 °C; no organic matter seems to remain at that temperature.

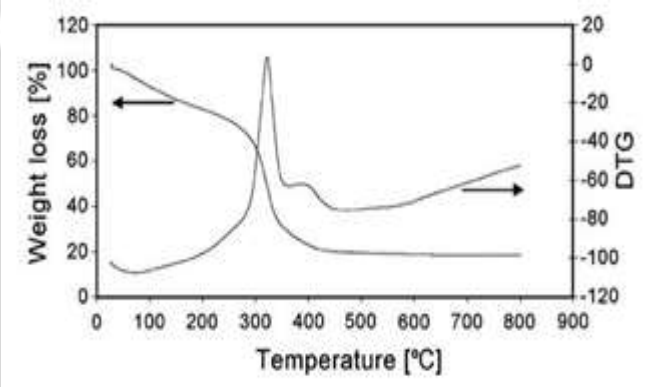

Figure 2. TGA-DTA curves of ZT gel precursor under air

The dilatometric curves of the powders are present-ed in Fig. 3. These experiments were performed for the ss-ZT powder annealed at 800 °C and the sg-ZT powders annealed at different temperatures. The shrinkage of the sg-ZT is not completed at 1150 °C, whereas, the ss-ZT shrinkage ends at 1150 °C.

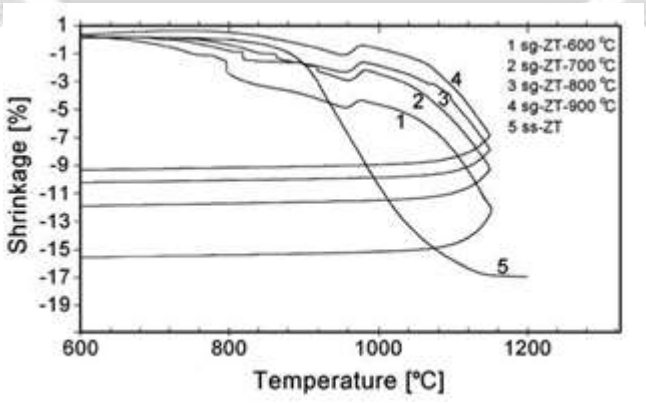

Figure 3. Shrinkage curves versus temperature of sg-ZT heat treated at different temperatures

5. CONCLUSION

In this paper two main advantages of the sol-gel method were highlighted: the low crystallization temperature (600 °C) and the high purity of the sg-ZT powders. The crystalline size of the sg-ZT powders was moreover very small. However, a drawback was the agglomeration of the powder. This phenomenon has a detrimental influence on the densification of the ceramics. Three techniques of deagglomeration were investigated, ultrasonication, pulverisation and attri-tion milling of which attrition milling was the most efficient. The sg- ZT-attr powder had fewer agglomer-ates, making the densification of the ceramic easier.

6. REFERENCES

[1] Feng Gao et. al, (2021),” (Ba, Sr) TiO3/polymer dielectric composites–progress and perspective” https://doi.org/10.1016/j.pmatsci.2021.100813

[2] Jyoti Rani et. al, (2021),” Exploring magnetoelectric coupling in trilayer [Ba (Zr0.2Ti0.8) O3-0.5(Ba0.7Ca0.3) TiO3]/ CoFe2O4/ [Ba (Zr0.2Ti0.8) O3- 0.5(Ba0.7Ca0.3) TiO3] thin film” https://doi.org/10.1016/j.jallcom.2020.157702

[3] G.M. Rashwan et. al, (2021),” Preparation and Characterization and Dielectric Properties of (Ba0.95Ca0.05) TiO3 Ceramic Material” Int. J. Thin. Film. Sci. Tec.10, No. 3, 127-135 (2021) http://dx.doi.org/10.18576/ijtfst/100301

[4] MD. Parvez Ahmad et. al, (2020),” Effect of carbon-doping on structural and dielectric properties of zinc oxide” Vol. 10, No. 04, 2050017 (2020) https://doi.org/10.1142/S2010135X20500174

[5] Kumari, Naveen & Kumar, Vinod & Singh, Shiwa Kant. (2014). Synthesis, structural and dielectric properties of Cr3+ substituted Fe3O4 nano-particles. Ceramics International. 40. 12199. 10.1016/j.ceramint.2014.04.061.

[6] A. Priya, E. Sinha, and S. K. Rout, “Structural, optical and microwave dielectric properties of BaS_xSrxWO4 ceramics prepared by solid state reaction route,” Solid State Sci., 20, 40–45, 2013.

[7] M. J. Gázquez, J. P. Bolívar, R. Garcia-tenorio, and F. Vaca, “A Review of the Production Cycle of Titanium Dioxide Pigment.,”. May, 441–458, 2014

[8] O. A. Ramdasi, S. G. Kakade, R. C. Kambale, and Y. D. Kolekar, “Ferroelectric and Dielectric Properties of BT based Lead Free Ceramics,” Res. J. Mater. Sci., 4(3), 7–9, 2016

[9] Q. Yue, L. Luo, X. Jiang, W. Li, and J. Zhou, “Aging effect of Mn-doped Ba0.77Ca0.23TiO3 ceramics,” J. Alloys Compd.,610,276–280,2014, doi: 10.1016/j.jallcom.2014.05.003.

[10] Q. Zhang, J. Zhai, Q. Ben, X. Yu, and X. Yao, “Enhanced microwave dielectric properties of Ba0.4Sr0.6TiO3 ceramics doping by metal Fe powders,” J. Appl. Phys.,112(10), 104104, Nov. 2012, Doi: 10.1063/1.4766276.

[11] M. Mostafa, K. Ebnalwaled, H. A. Saied, and R. Roshdy, “Effect of laser beam on structural, optical, and electrical properties of BaTiO3 nanoparticles during sol-gel preparation,” J. Korean Ceram. Soc., 55(6), 581–589, 2018, doi: 10.4191/kcers.2018.55.6.04

[12] K. Momma and F. Izumi, “{\it VESTA3} for three-dimensional visualization of crystal, volumetric and morphology data,” J. Appl. Crystallography., 44(6), 1272–1276, 2011, doi: 10.1107/S0021889811038970.

[13] G. M. R. M.K. Gerges, M. Mostafa, “Structural, optical and electrical properties of PbTiO3 nanoparticles prepared by Sol-Gel method,” Ijlret., 2(4), 42–49, 2016.

[14] Aal, A. Abdel, et al. "FTIR study of nanostructure perovskite BaTiO3 doped with both Fe3+ and Ni2+ ions prepared by sol-gel technique." Acta Phys. Pol., A 126.6, 1318-1322, 2014.

[15] M. Mostafa, Z. A. Alrowaili, G. M. Rashwan, and M. K. Gerges, “Ferroelectric behavior and spectroscopic properties of La-Modified lead titanate nanoparticles prepared by a solgelmethod,” Heliyon.,6(2),2020, doi: 10.1016/j.heliyon. 2020.e03389.